arXiv:0708.2335v1 [physics.optics] 17 Aug 2007

2D shift of the centre of gravity of the light beam carrying orbital angular momentum, which accompanies reflection from a lossy medium

V.G.Fedoseyev
Institute of Physics, University of Tartu,
Riia 142, 51014 Tartu, Estonia

February 5, 2008

Abstract

It is shown that after reflection from a lossy medium the s- or p-polarized paraxial light beam carrying the orbital angular momentum suffers the 2D shift of the beam's centre of gravity relative the geometric optic axis. The mutually orthogonal components of this shift are expressed through the real and imaginary parts of the common complex quantity. The features of the 2D vector, which describes the shift, are analyzed.

PACS: 42.25.-p; 42.25.Gy; 42.60.Jf
Keywords: orbital angular momentum, reflection, transverse shift, Goos-Hänchen shift

I. Introduction

In the communication [1], a new nonspecular effect, which accompanies the process of partial reflection of a paraxial light beam at a plane sharp interface of two isotropic transparent media, has been predicted. It was shown that,

if the incident beam carries the intrinsic orbital angular momentum (OAM), the centre of gravity of the reflected beam (CGRB) suffers a transverse shift (TS), i.e. the shift perpendicular to the plane of incidence. Bekshaev and Popov [2] considered the OAM-dependent TS using the method of transformation of space-angle intensity moments during the interaction of the beam with a layered structure. Bliokh compared this effect with the phenomena accompanying transformation of the OAM in the course of propagation of a beam in the smoothly inhomogeneous media [3].

Unlike the previously known, spin-dependent TS (see, for instance, [4-9] and references therein), the OAM-dependent TS can take place, when the incident beam is *s*- or *p*-polarized. This effect appears because the electromagnetic energy inside the beam is redistributed after reflection in such a way that the intensity increases at one side of the incidence plane and decreases at the other [10,11]; in the regular region, the respective corrections are proportional to the ratio of the wavelength to the radius of the beam.

The magnitude of the OAM-dependent TS is, if an angle of incidence is not close to the critical angle for total reflection or (for *p*-polarization) to the Brewster angle, rather small: it is of the order of the wavelength or less. But, at the present, the optical method has been developed, which permit to detect the positions of the objects with nanometer-scale precision (see, for instance, [12] and references therein). This method has been used by Dasgupta and Gupta [13] in order to define the OAM-dependent TSs of the CGRB in the wide region of the angles of incidence, the authors of [13] have reported a good agreement between their experimental results and the predicted values of the TSs.

Recently, Okudo and Sasada have observed the redistribution of the electromagnetic energy inside the beam carrying the OAM after its reflection from the transparent medium [11]. Their experiments were carried out in a situation, where the angle of incidence was close to the critical angle for total reflection. In this region, the magnitude of the effect increases significantly, so the energy redistribution becomes visible (see Figs. 3 and 4 in [11]). The authors of [11] have performed the respective numerical simulations, which turned out to be in a good agreement with the experimental results. The OAM-dependent TS was not calculated in [11], but this calculation was possible [14].

Basing on the results of [11] and [13] one can conclude that the OAM-dependent TS of the CGRB is a quantity, which can be detected experimen-

tally, so, this effect can be used in order to investigate some features of the light and the matter. Thus, this effect is connected with the rotation motion of the electromagnetic energy inside the incident beam [15-17]; hence, if the OAM-dependent TS of the CGRB is detected, one can conclude that such a motion takes place.

In this communication, we shall consider the OAM-dependent TS of the CGRB together with another shift, which is parallel to the plane of incidence and which corresponds to the well-known Goos-Hänchen shift (see, for instance, [5,8,9,18-21] and references therein); these shifts are of the same scale, moreover, they have a common origin. By this, we will assume that the reflecting medium may be lossy.

II. Geometry of reflection

We shall consider the reflection of a monochromatic light beam at a plane interface of two semi-infinite isotropic, nondispersive, and nonmagnetic media. The scheme of the process is shown in Fig. 1. The position of the interface is defined by equation $\hat{\mathbf{N}}\cdot\boldsymbol{\rho}=0$, where $\boldsymbol{\rho}$ is the 3D radius vector, and $\hat{\mathbf{N}}$ is the unit normal to the interface directed from the first (incident) medium to the second (reflecting) one. The dielectric constants of the media in the upper half-space ($\hat{\mathbf{N}}\cdot\boldsymbol{\rho}<0$) and the lower half-space ($\hat{\mathbf{N}}\cdot\boldsymbol{\rho}>0$) will be denoted by ϵ_1 and ϵ_2, respectively. The relative dielectric constant $\epsilon=\epsilon_2/\epsilon_1$. The first medium is assumed to be transparent, while the second medium may be lossy, i.e. we assume that ϵ_1 is positive, while ϵ_2 and, as a consequence, ϵ may be complex, so, in general case, $\epsilon=\epsilon'+i\epsilon''$. Here and further on, the prime and double prime stand for the real and imaginary parts of a quantity.

Throughout this paper, we shall use the superscripts i and r for indicating the quantities characteristic of the incident and of the reflected beams, respectively; the superscript a will be used in order to designate an arbitrary (incident or reflected) beam, so, a=i or r. We shall employ two coordinate systems connected with the incident and the reflected beams, these systems will be termed the i- and r-systems.

In the i-system, the $z^{(i)}$ axis is assumed to coincide with the incident beam's axis. This axis and the unit vector $\hat{\mathbf{N}}$ define the position of the beam's plane of incidence in 3D space; the angle θ between the unit vectors $\hat{\mathbf{N}}$ and $\hat{\mathbf{z}}^{(i)}$ is the beam's angle of incidence: $\theta=\arccos(\hat{\mathbf{N}}\cdot\hat{\mathbf{z}}^{(i)})$. The coordinate

origin O is taken to be the point of intersection of the incident beam axis with the interface. In the r-system, the $z^{(r)}$ axis is assumed to coincide with the geometric optic (GO) axis of the reflected beam. The latter is defined as a ray, which is intersected by the interface at the coordinate origin, and whose direction is characterized by the unit vector $\hat{\mathbf{z}}^{(r)}$, which is related to $\hat{\mathbf{z}}^{(i)}$ through the Snell's law and is written as follows: $\hat{\mathbf{z}}^{(r)} = \hat{\mathbf{z}}^{(i)} - 2(\hat{\mathbf{N}} \cdot \hat{\mathbf{z}}^{(i)})\hat{\mathbf{N}}$. The beam's angle of reflection $\theta^{(r)} = \arccos(\hat{\mathbf{N}} \cdot \hat{\mathbf{z}}^{(r)}) = \pi - \theta$.

The y axis in every system is defined to be perpendicular to the plane of incidence, it is characterized by the unit vector $\hat{\mathbf{y}} = \hat{\mathbf{N}} \times \hat{\mathbf{z}}^{(i)} / |\hat{\mathbf{N}} \times \hat{\mathbf{z}}^{(i)}|$; this axis (the transverse one) is common for both systems. The direction of the $x^{(a)}$ axis of the a-system, which lies in the plane of incidence, is defined by the unit vector $\hat{\mathbf{x}}^{(a)} = \hat{\mathbf{y}} \times \hat{\mathbf{z}}^{(a)}$.

In the a- system, the 3D radius-vector is represented as follows:

$$\boldsymbol{\rho} = z^{(a)}\hat{\mathbf{z}}^{(a)} + \mathbf{u}^{(a)} \ , \tag{1}$$

where $\mathbf{u}^{(i)}$ and $\mathbf{u}^{(r)}$ are the 2D planar radius vectors lying in the planes, which are perpendicular to the axis of the incident beam and to the GO axis of the reflected beam, respectively,

$$\mathbf{u}^{(a)} = x^{(a)}\hat{\mathbf{x}}^{(a)} + y\hat{\mathbf{y}} \ . \tag{2}$$

III. Incident and reflected fields

Let us assume that the incident beam is paraxial, that it carries the well-defined OAM ([22,23]), and that it is mainly s- or p-polarized. Due to first assumption, the relation

$$\lambda / \pi b \ll 1 \ , \tag{3}$$

must be fulfilled, where λ is the wavelength of light in the first medium, and b is the beam radius.

The electrical field vector of the incident beam under consideration can be written, in its own coordinate system, as follows [24]:

$$\mathbf{E}_\alpha^{(i)}(\boldsymbol{\rho}) \simeq \left[\hat{\mathbf{e}}_\alpha^{(i)} - i\frac{\lambda}{2\pi}\hat{\mathbf{z}}^{(i)} \left(\hat{\mathbf{e}}_\alpha^{(i)} \cdot \frac{d}{d\mathbf{u}^{(i)}} \right) \right] F^{(i)}(\boldsymbol{\rho}) + c.c. \ , \tag{4}$$

where the subscript α denotes the polarization of the incident beam ($\alpha = s$ or p), while $\hat{\mathbf{e}}_\alpha^{(i)}$ is the polarization vector: $\hat{\mathbf{e}}_s^{(i)} \equiv \hat{\mathbf{y}}$, and $\hat{\mathbf{e}}_p^{(i)} \equiv \hat{\mathbf{x}}^{(i)}$. The

function $F^{(i)}(\boldsymbol{\rho})$ in the right-hand side of Eq. (4) can be represented as a product of two terms:

$$F^{(i)}(\boldsymbol{\rho}) = f(u^{(i)}, z^{(i)}) \exp(-il\varphi^{(i)}) \ , \tag{5}$$

where l is the azimuthal index ($l = 0, \pm 1, \pm 2 ...$), and $\varphi^{(i)}$ is the azimuth obtained from the relation: $\tan \varphi^{(i)} = y/x^{(i)}$. The term $f(u^{(i)}, z^{(i)})$ does not depend on $\varphi^{(i)}$, for instance, it may be given by the Laguerre-Gaussian function or, like in [11], by a superposition of such functions. For the forthcoming analysis , the specification of $f(u^{(i)}, z^{(i)})$ is not necessary. The time dependence of $\mathbf{E}^{(i)}$ is suppressed.

The electrical field vector of the reflected beam $\mathbf{E}^{(r)}(\boldsymbol{\rho})$ is calculated in the standard way (see, for instance, [6,10,18]). First, the 2D Fourier transform of the function $F^{(i)}(\boldsymbol{\rho})$ with respect to the coordinates $x^{(i)}$ and y is to be performed. Then the vector $\mathbf{E}^{(i)}(\boldsymbol{\rho})$ will be represented as a superposition of the plane waves. Next, the Snell and Fresnel laws should be applied to the particular plane waves. After that, the reverse 2D Fourier transform should be performed.

Let us denote the angle of incidence of the particular plane wave inside the incident beam by $\theta^{(ip)}$. For the actual waves constituting a paraxial beam, $|\theta^{(ip)} - \theta| \sim \lambda/b \ll 1$. So, one can expand the particular Fresnel field reflection coefficients in the truncated power series with respect to $\theta^{(ip)} - \theta$. When the second medium is transparent, and $\epsilon' < 1$, such an expansion can be substantiated, if θ is not too close to the critical angle for total reflection given by

$$\theta^{(c)} = \arcsin \sqrt{\epsilon'} \ , \tag{6}$$

i.e. if the condition

$$|\theta - \theta^{(c)}| \gg \lambda/b, \quad if\ \epsilon' < 1, \ \ and\ \ \epsilon'' \to -0 \ , \tag{7}$$

is fulfilled. Again, in the case of p-polarization, the expansion is substantiated, if θ is not too close to the Brewster angle given by

$$\theta^{(B)} = \arctan \sqrt{\epsilon'} \ , \tag{8}$$

i.e. if the condition

$$|\theta - \theta^{(B)}| \gg \lambda/b, \quad if\ \alpha \equiv p, \ \ and\ \epsilon'' \to -0 \ , \tag{9}$$

is fulfilled. But, when

$$|\epsilon''| \gg \lambda/b \;, \tag{10}$$

the series expansion is justified at any θ.

Let us restrict ourselves with the near-field region (in this case the possible angular shifts can be excluded from consideration), i.e. let us assume that

$$z^{(r)} \ll \pi b^2/\lambda \;. \tag{11}$$

If the restrictions (11), and (7), (9) or (10) are fulfilled, it is possible to retain only the zero-order and first-order terms in the power series expansion.

Performing the operations, which are mentioned in three by last paragraph, one obtains the following expression for the electrical field vector of the reflected beam written in its coordinate system:

$$\mathbf{E}_\alpha^{(r)}(\boldsymbol{\rho}) \simeq r_\alpha(\theta)\left[\hat{\mathbf{e}}_\alpha^{(r)}\left(1 + iQ_\alpha(\theta)\frac{\lambda}{2\pi}\frac{d}{dx^{(r)}}\right) - i\frac{\lambda}{2\pi}\hat{\mathbf{z}}^{(r)}\left(\hat{\mathbf{e}}_\alpha^{(r)}\cdot\frac{d}{d\mathbf{u}^{(r)}}\right)\right] f(u^{(r)}, z^{(r)})\exp(il\varphi^{(r)}) + c.c. \;, \tag{12}$$

where $\hat{\mathbf{e}}_s^{(r)} \equiv \hat{\mathbf{y}}$, $\hat{\mathbf{e}}_p^{(r)} \equiv \hat{\mathbf{x}}^{(r)}$, and $\tan\varphi^{(r)} = y/x^{(r)}$. The quantity $Q_\alpha(\theta)$ in the right-hand side of Eq. (12) is as follows:

$$Q_\alpha(\theta) = -\frac{1}{2}\frac{d}{d\vartheta}\left(\ln r_\alpha(\vartheta)\right)\Big|_{\vartheta=\theta} \;, \tag{13}$$

where $r_\alpha(\vartheta)$ is the familiar Fresnel's field reflection coefficient of the α-polarized plane wave, which is incident at an angle ϑ [25]:

$$r_s(\vartheta) = -\frac{\sin(\vartheta-\tau)}{\sin(\vartheta+\tau)} \;, \quad r_p(\vartheta) = \frac{\tan(\vartheta-\tau)}{\tan(\vartheta+\tau)} \;, \tag{14}$$

and where τ is the angle of refraction given by the relation $\sqrt{\epsilon}\sin\tau = \sin\vartheta$, in a general case τ is complex. The dependence of the vector $\mathbf{E}_\alpha^{(r)}(\boldsymbol{\rho})$ on θ is not explicitly written down.

Basing on Eqs. (13) and (14), the calculations of the factor $Q_s(\theta)$ and $Q_p(\theta)$ are straightforward, the results are as follows [10]:

$$Q_s(\theta) = -\frac{\sin\theta}{(\epsilon - \sin^2\theta)^{1/2}} \;, \tag{15}$$

and

$$Q_p(\theta) = \frac{Q_s(\theta)}{\epsilon^{-1}\sin^2\theta - \cos^2\theta} \ . \tag{16}$$

Generally, $Q_\alpha(\theta)$ is a complex quantity, its real and imaginary parts are caused by the dependence on θ of the amplitude and the phase, respectively, of the Fresnel's field reflection coefficient $r_\alpha(\theta)$. The expressions (15) and (16) are in accordance with the respective expression obtained in [21] (see Eq. (29)).

The magnetic field vector of the reflected beam $\mathbf{H}_\alpha^{(r)}(\boldsymbol{\rho})$ is obtained by means of the Faraday's law.

IV. 2D shift of the CGRB

A. Definition and results of calculations. Let us select the plane, which is perpendicular to the GO axis of the reflected beam (the output plane in Fig. 1). The position of the CGRB on this plane (see Fig. 2) is given by the 2D vector

$$\mathbf{U}_\alpha(\theta) = \frac{1}{W_\alpha^{(r)}} \int \mathbf{u}^{(r)} w_\alpha^{(r)}(\boldsymbol{\rho}) d\mathbf{u}^{(r)} \ , \tag{17}$$

where $w_\alpha^{(r)}(\boldsymbol{\rho})$ is the electromagnetic energy density inside the reflected beam

$$w_\alpha^{(r)}(\boldsymbol{\rho}) = \frac{1}{8\pi}\left[\epsilon_1 \left(\mathbf{E}_\alpha^{(r)}(\boldsymbol{\rho})\right)^2 + \left(\mathbf{H}_\alpha^{(r)}(\boldsymbol{\rho})\right)^2\right] \ , \tag{18}$$

and

$$W_\alpha^{(r)} = \int w_\alpha^{(r)}(\boldsymbol{\rho}) d\mathbf{u}^{(r)} \ . \tag{19}$$

As the GO axis intersects the output plane at the point $\mathbf{u}^{(r)} = 0$, the vector $\mathbf{U}_\alpha(\theta)$, which is shown in Fig. 2, describes the 2D shift of the CGRB relative to this axis.

Let impose the following restriction on the axial coordinate of the output plane:

$$z^{(r)} \gg b/\sin(2\theta) \ . \tag{20}$$

If the restriction (20) is fulfilled, the reflected field on the output plane is not overlapped with the incident field. Again, $w_\alpha^{(r)}(\mathbf{u}^{(r)})$ is negligible at the line of intersection of the output plane and the interface; in this case, the lower limit of integration over $x^{(r)}$ in Eqs. (17) and (19) can be substituted

by $-\infty$. Once this substitution is made and the expression (12) for $\mathbf{E}_\alpha^{(r)}(\boldsymbol{\rho})$ and respective expression for $\mathbf{H}_\alpha^{(r)}(\boldsymbol{\rho})$ obtained by means of the Faraday's law are used, the calculation of $\mathbf{U}_\alpha(\theta)^{(r)}$ is straightforward. In the first-order approximation with respect to λ/b, one obtains

$$\mathbf{U}_\alpha(\theta) = X_\alpha(\theta)\hat{\mathbf{x}}^{(r)} + Y_\alpha(\theta)\hat{\mathbf{y}} \;, \tag{21}$$

where

$$X_\alpha(\theta) = Q''_\alpha(\theta)\frac{\lambda}{\pi} \;, \tag{22}$$

and

$$Y_\alpha(\theta) = lQ'_\alpha(\theta)\frac{\lambda}{\pi} \;. \tag{23}$$

B. Analysis. As follows from Eq. (21), the shift of the CGRB relative to the GO axis is, in a general case, described by the 2D vector $\mathbf{U}_\alpha(\theta)$ on the output plane. Its $x^{(r)}$-component ($X_\alpha(\theta)$) does not depend on l, while the y-component ($Y_\alpha(\theta)$) is proportional to l. Apart from the factor l, the functions $X_\alpha(\theta)$ and $Y_\alpha(\theta)$ are represented by the imaginary and real parts of the same complex quantity, it is in spite of the fact that the mechanisms of the appearances of the orthogonal components of the 2D shift are different [10,26]. Figs. 3(a,b) illustrate dependence of the functions Q'_α and Q''_α on θ for different values of ϵ' and ϵ''.

When the second medium is transparent, the vector $\mathbf{U}_\alpha(\theta)$ is parallel either to the $x^{(r)}$ axis (in the total-reflection regime) or to the y axis (in the partial-reflection regime). In this case, the expression (21) reduces to the one of the previously obtained expressions, either for the Goos-Hänchen shift [27] or for the OAM-dependent TS of the CGRB [1]. When the second medium is lossy, the vector $\mathbf{U}_\alpha(\theta)$ is inclined to the coordinate axes, as is shown in Fig. 2. By this, the direction of $\mathbf{U}_\alpha(\theta)$ depends on the angle of incidence, and the vector $\mathbf{U}_\alpha(\theta)$ rotates around the coordinate origin, i.e. around the CO axis, when θ changes.

The direction of $\mathbf{U}_\alpha(\theta)$ is defined by its azimuth $\Gamma_\alpha(\theta)$, which is given by the equation: $\tan\Gamma_\alpha(\theta) = Y_\alpha(\theta)/X_\alpha(\theta)$. Substituting in its right-hand side Eqs. (22) and (23) one obtains the relation between the azimuth $\Gamma_\alpha(\theta)$ and the argument of the complex quantity $Q_\alpha(\theta)$, which is defined by $\gamma_\alpha(\theta) = (\ln Q_\alpha(\theta))''$); this relation looks as follows :

$$\tan\Gamma_\alpha(\theta) = l/\tan\gamma_\alpha(\theta) \;. \tag{24}$$

In particular, if $l = \pm 1$,

$$\Gamma_\alpha(\theta) = l(\frac{\pi}{2} - \gamma_\alpha(\theta)) \ . \tag{25}$$

As for the arguments $\gamma_s(\theta)$ and $\gamma_p(\theta)$, they are obtained from the expressions (15) and (16):

$$\gamma_s(\theta) = \frac{1}{2}\text{arccotan}\left(\frac{\epsilon' - \sin^2\theta}{|\epsilon''|}\right) - \pi \ , \tag{26}$$

and

$$\gamma_p(\theta) = \gamma_s(\theta) - \text{arccotan}\left(\frac{\epsilon' - |\epsilon|^2\cot^2\theta}{|\epsilon''|}\right) \ . \tag{27}$$

Basing on Eqs. (24)-(27) one can make the following conclusions about the orientation of the vectors $\mathbf{U}_s(\theta)$ and $\mathbf{U}_p(\theta)$. As follows from Eq. (26), $-\pi/2 > \gamma_s(\theta) > -\pi$ at any θ, i.e. $Q_s(\theta)$ lies in the third quadrant of the complex plane; as a consequence, the vector $\mathbf{U}_s(\theta)$ (see Eq. (24))lies in the third quadrant of the output plane ($X_s(\theta) < 0, Y_s(\theta) < 0$), if $l > 0$, and in the second quadrant($X_s(\theta) < 0, Y_s(\theta) > 0$), if $l < 0$. The positions of $Q_p(\theta)$ on the complex plane and of the vector $\mathbf{U}_p(\theta)$ on the output plane, unlike of $Q_s(\theta)$ and $\mathbf{U}_s(\theta)$, are not contained within one quadrant, when θ changes from 0 to $\pi/2$. At small θ the direction of the vector $\mathbf{U}_p(\theta)$ is approximately opposite with respect to the direction of the vector $\mathbf{U}_s(\theta)$. As θ increases, the sign of $Y_p(\theta)$ changes once independent of the value of ϵ. The sign of $X_p(\theta)$ changes, if the condition

$$2\epsilon' > |\epsilon|^2 \tag{28}$$

is fulfilled. The numerical analysis of dependence of X on θ has been recently performed by

The angles, at which these changes take place, are obtained from the following equation:

$$|\epsilon|^2\cot^4\theta + 2(1 + \epsilon'|\epsilon|^{-2})\sin^2\theta - 3 = 0 \ . \tag{29}$$

If $\epsilon'' \to -0$ and $\epsilon' > 0$, the second term in the right-hand side of Eq. (27) have the jump discontinuity at the Brewster angle $\theta^{(B)}$, where γ_p changes abruptly by π. If in addition $\epsilon' < 1$, the $(\pi/2)$-jump of γ_s and γ_p takes place at the critical angle for total reflection $\theta^{(c)}$. Figs. 4(a,b) illustrate dependence of the functions Γ_p and Γ_s on θ for different values of ϵ and l.

The scale of the 2D shift is λ/π, but, if $|\epsilon''| \ll 1$, its magnitude increases significantly in the vicinity of the angle $\theta^{(c)}$ and, for p-polarization, in the vicinity of the angle $\theta^{(B)}$, these angles are given by Eqs. (6) and (8), respectively. Fig. 5 illustrates the behavior of the vector $\mathbf{U}_s(\theta)$ in the former domain, the behavior of the vector $\mathbf{U}_p(\theta)$ in this domain is similar (see further Eq. (30)). It is seen that, when $l \neq 0$, the effect of rotation of the vector $\mathbf{U}_\alpha(\theta)$ around the GO axis as well as change of its length in the process of the change of θ is pronounced. Again, if $|\epsilon''| \ll 1$, and $|\theta - \theta^{(c)}| \ll 1$, the position of the vector $\mathbf{U}_\alpha(\theta)$ is sensitive to small changes of the values of ϵ' and ϵ'' (see Figs. 6 and 7). If the above-mentioned conditions are fulfilled, the approximate expressions of the functions $Q'_\alpha(\theta)$ and $Q''_\alpha(\theta)$ look as follows:

$$Q_s^{';''}(\theta) = \epsilon' Q_p^{';''}(\theta) = -\left(\frac{\epsilon'}{2|\epsilon''|}\right)^{1/2} \left(\frac{(\Delta^2+1)^{1/2} \mp \Delta}{\Delta^2+1}\right)^{1/2} , \qquad (30)$$

where $\Delta = (\theta - \theta^{(c)}) \sin(2\theta^{(c)})/|\epsilon''|$, in (30) and further on the signs minus and plus stand for $Q'_\alpha(\theta)$ and $Q''_\alpha(\theta)$, respectively. Notice that, relative to the point $\theta = \theta^{(c)}$, i.e. to the point $\Delta = 0$, the functions $Q'_\alpha(\theta)$ and $Q''_\alpha(\theta)$ given by Eq. (30) are mutually symmetric. The magnitudes of these functions achieve the maximums at the symmetrical points $\Delta^{(\prime)}_{max}$ and $\Delta^{(\prime\prime)}_{max}$, respectively, given by $\Delta^{(\prime\prime)}_{max} = -\Delta^{(\prime)}_{max} = 1/\sqrt{3}$. By this, $Q'_s(\Delta^{(\prime)}_{max}) = Q''_s(\Delta^{(\prime\prime)}_{max}) = -(3/4)^{3/4}(\epsilon'/|\epsilon''|)^{1/2}$.

The behavior of the vector $\mathbf{U}_\alpha(\theta)$ in the vicinity of $\theta^{(B)}$ is shown in Fig. 8. Like in the previous case, the effect of rotation of this vector around the GO axis with the change of θ is pronounced in this domain; again, the position of $\mathbf{U}_p(\theta)$ is sensitive to small changes of the values of ϵ' and ϵ'' (these effects are not demonstrated). When $|\epsilon''| \ll 1$, and $|\theta - \theta^{(B)}| \ll 1$,

$$Q_p(\theta) \simeq -\frac{1}{2}\left(\theta - \theta^{(B)} + i\frac{|\epsilon''|}{2(1+\epsilon')\sqrt{\epsilon'}}\right)^{-1} , \qquad (31)$$

while $|Q_s(\theta)|$ is small in comparison with $|Q_p(\theta)|$, namely, $Q'_s(\theta) \simeq -1/\sqrt{\epsilon'}$, and $|Q''_s(\theta)| \ll |Q'_s(\theta)|$.

The numerical analysis of dependence of Goos-Hänchen shift, i.e. of the quantity X, on θ has been recently performed by Lai *et al.* The authors of [21] have paid special attention to the behavior of this shift in the vicinity of the Brewster dip. Eq. (31) shows that, if $|\epsilon''| \ll 1$, the function $X_p(\theta)$ is approximated in this region by the Lorentz curve.

C. Relative p-s shift. Detection of the shift of the CGRB of the s- or p-polarized beam requires a careful determination of the position of the GO axis. The latter procedure can meet the difficulties. One can escape these difficulties by operating with the difference of the shifts of two beams having the orthogonal polarizations, such a scheme has been realized in the experiments by Dasgupta and Gupta [13]. In [13], the initial beam was randomly polarized, and the s- or p-polarization were selected by means of rotation of a linear polarizer. The other elements of the set-up were kept motionless.

¿From Eqs. (17) and (19), the difference between the centres of gravity of the respective reflected beams

$$\mathbf{U}_{ps}(\theta) \equiv \mathbf{U}_p(\theta) - \mathbf{U}_s(\theta) = \frac{1}{W_s^{(r)} W_p^{(r)}} \int \mathbf{u}^{(r)} G^{(r)}(\mathbf{u}^{(r)}) d\mathbf{u}^{(r)}, \qquad (32)$$

where $G^{(r)}(\mathbf{u}^{(r)})$ is the cross-correlation function,

$$G^{(r)}(\mathbf{u}^{(r)}) = \int w_p^{(r)}(\mathbf{u}^{(r)} + \mathbf{v}^{(r)}) w_s^{(r)}(\mathbf{v}^{(r)}) d\mathbf{v}^{(r)} \,, \qquad (33)$$

and where $\mathbf{v}^{(r)}$ is, like $\mathbf{u}^{(r)}$, the 2D radius vector lying in the plane perpendicular to $\hat{\mathbf{e}}_z^{(r)}$. The vector $\mathbf{U}_{ps}(\theta)$, unlike the vectors $\mathbf{U}_s(\theta)$ and $\mathbf{U}_p(\theta)$, does not depend on the position of the GO axis.

Let us consider the case, when both incident beams have the common axes and, as a consequence, both reflected beams have the common GO axes. Such a situation takes place, for instance, if, within the scheme of the experiment [13], the rotation of the polarizer do not affect the position of the axis of the incident beam. In this case

$$\mathbf{U}_{ps}^{(r)}(\theta) = \left(Q''_{ps}(\theta) \hat{\mathbf{x}}^{(r)} + l Q'_{ps}(\theta) \hat{\mathbf{y}} \right) \frac{\lambda}{\pi} \,, \qquad (34)$$

where

$$Q_{ps}(\theta) = Q_p(\theta) - Q_s(\theta) \,. \qquad (35)$$

Generalization of the expression (34) for the case, when the axes of the mutually orthogonally polarized incident beams are parallel, is straightforward.

V. Conclusions

When the s- or p-polarized paraxial light beam, which carries the OAM, is reflected from the lossy medium, two mutually orthogonal shifts of the CGRB to scale λ appear; so, in the near-field region, the total shift is described by the 2D vector $\mathbf{U}_s(\theta)$ or $\mathbf{U}_p(\theta)$ on the output plane. The vector $\mathbf{U}_\alpha(\theta)$, with $\alpha = s$ or p, is given by Eq. (21) and its orthogonal components are given by Eqs. (22) and (23). The second medium is transparent, these expressions are correct, if conditions (7) and (9) are fulfilled. The second medium is lossy, and condition (10) for $|\epsilon''|$ is fulfilled, the above-mentioned expressions are correct at any θ.

The vectors $\mathbf{U}_s(\theta)$ and $\mathbf{U}_p(\theta)$ are defined relative the GO axis of the reflected beam; the difference between them (the vector $\mathbf{U}_{ps}(\theta) \equiv \mathbf{U}_p(\theta) - \mathbf{U}_s(\theta)$) does not depend on the position of the GO axis, it is expressed through the cross-correlation function of two energy distributions across the output plane (Eqs. (32) and (33)).

The component of the vector $\mathbf{U}_\alpha(\theta)$, which is parallel to the plane of incidence ($X_\alpha(\theta)$) corresponds to the Goos-Hänchen shift, it does not depend on the azimuthal index l. The transverse component $Y_\alpha(\theta)$, which represents the OAM-dependent TS of the CGRB, is proportional to l. Apart of the factor l, the components $X_\alpha(\theta)$ and $Y_\alpha(\theta)$ are given by the imaginary and real parts of the common quantity.

Redistribution of the electromagnetic energy inside the reflected beam, which entails the OAM-dependent TS of the CGRB, is connected with the rotation energy motion inside the incident beam [15-17]; hence, if a deflection of the vector $\mathbf{U}_\alpha(\theta)$ from the $x^{(r)}$ axis is detected, one can conclude that such a motion takes place.

In the case of s-polarization the signs of both components of 2D shift do not depend on θ: the vector $\mathbf{U}_s(\theta)$ lies in the third quadrant of the output plane, if $l > 0$, and in the second quadrant, if $l < 0$. On the contrary, the positions of the vector $\mathbf{U}_p(\theta)$ on the output plane is not contained within one quadrant when θ changes from 0 up to $\pi/2$. The azimuths of the vectors $\mathbf{U}_s(\theta)$ and $\mathbf{U}_p(\theta)$ are given by Eqs. (24)-(27). At small θ the directions of these vectors are approximately opposite . As θ increases, the sign of $Y_p(\theta)$ changes one time independent of the value of ϵ, while the sign of $X_p(\theta)$ changes, if the condition (28) is fulfilled. Generally, when θ changes, the rotation of the vector $\mathbf{U}_\alpha(\theta)$ around the GO axis as well as the change of

its length takes place; these effects are most pronounced if $|\epsilon''| \ll 1$ and θ is close to $\theta^{(c)}$ or, for $\alpha = p$, to $\theta^{(B)}$. In these domains, the quantity $Q_\alpha(\theta)$ is approximated by expression (30) or (31). In the vicinity of $\theta^{(c)}$, the dependence of the vector $\mathbf{U}_s(\theta)$ on θ is shown in Fig. 5, the behaviors of the vectors $\mathbf{U}_p(\theta)$ and $\mathbf{U}_{ps}(\theta)$ are, due to the left relation in (30), similar to behavior of $\mathbf{U}_s(\theta)$. In the vicinity of $\theta^{(B)}$, the dependence of the vector $\mathbf{U}_p(\theta)$ on θ is shown in Fig. 8.

In the above-mentioned domains, the position of the vector $\mathbf{U}_\alpha(\theta)$ is sensitive to small changes of the values of ϵ' and ϵ'' (see Figs. 6 and 7). This may be used as a tool for the investigation of the small changes of the dielectric constants of the media. Again, in view of this fact, one can await that, if the reflecting medium is taken to be nonlinear, the dependence of the position of the vector $\mathbf{U}_\alpha(\theta)$ on the light intensity should be pronounced in the above-mentioned domains.

1 Acknowledgment.

The author thanks H.Sasada for valuable correspondence. This work was supported by Estonian Science Foundation (grant No. 6534)

References

[1] Fedoseyev V G 2001 *Opt. Commun.* **193** 9-18

[2] Bekshaev A Yu and Popov A Y 2002 *Proc. SPIE* **4607** 90-8

[3] Bliokh K Yu 2006 *Phys. Rev. Lett.* **97** 043901

[4] Fedorov F I 1977 *Zh. Prikl. Spektrosk.* **27** 580-8

[5] Fedoseyev 1991 V G *Opt.Spectrosk.* **71** 992-7 [*1991 Opt. Spectrosc. (USSR)*] **71** 570

[6] Nasalski W 1996 *J. Opt. Soc. Am. A* **13** 172-81

[7] Pillon F, Gilles H, Sylvain G, and Laroche M 2005 *J. Opt. Soc. Am. B* **22** 1290-9

[8] Onoda M, Murakami S, and Nagaosa N 2006 *Phys. Rev. E* **74** 066610

[9] Bliokh K Yu and Bliokh Yu P 2007 *Phys. Rev. E* **75** 066609

[10] Fedoseyev V G 2001 *Proc. SPIE* **4403** 90-7

[11] Okuda H and Sasada H 2006 *Opt. Express* **14** 8393-402

[12] Gelles J, Schnapp B, and Sheets M P 1988 *Nature* **331** 450-3

[13] Dasgupta R and Gupta P K 2006 *Opt. Commun.* **257** 91-6

[14] Sasada H (*private communication*)

[15] Marienko I G, Pasko V A, Slyusar, Soskin M S, and Vasnetsov M V 2002 *Opt. Commun.* **213** 1-11

[16] Fedoseyev V G 2002 *Abstracts of the International "Seminar Day on Difraction-2002, St.Petersburg, Russia"* 28

[17] Fedoseyev V G 2004 *Proc. SPIE* **5481** 154-9

[18] Hsue C W and Tamir T 1984 *Opt. Commun.* **49** 383-7

[19] Porras M A 1997 *Opt. Commun.* **135** 369-377

[20] Shadrivof I V, Zharov A A, and Kivshar Yu S 2003 *Appl. Phys. Lett.* **83** 2713-5

[21] H.M. Lai, Chan S W, and Wong W H 2006 *J. Opt. Soc. Am. A* **23** 3208-16.

[22] Allen L, Beijersbergen M W, Spreeuw R J, and Woerdman J P 1992 *Phys. Rev. A* **45** 8185-9

[23] Allen L, Barnet S M, and Padgett M J (Ed.) 2003 *Optical angular momentum, Institute of Physics Publishing, Bristol and Philadelfia*

[24] Haus 1984 H A *Waves and Fields in Optoelectronics, Prentice-Hall, Englewood Cliffs, New Jersey*

[25] Born M and Wolf E 1965 *Principles of Optics, 3rd ed. Pergamon, Oxford, U.K.*

[26] Fedoseyev V G *(to be published)*

[27] Artman 1948 K *Ann. Phys. (Leipzig)* **2** 87-102

FIGURE CAPTIONS.

Fig. 1. Geometry of reflection.

Fig. 2. Position of the vector $\mathbf{U}$ on the output plane, the azimuth Γ is shown, the subscripts α are suppressed in this figure. The numerals 1, 2, 3, and 4 denote the quadrant' numbers.

Fig. 3(a). Q'_α (thin curves) and Q''_α (thick curves) versus θ. $\epsilon' = 2$; solid lines correspond to $\epsilon'' = -0.001$, and dashed lines to $\epsilon'' = -0.5$.

Fig. 3(b). Same as in Fig. 3(a) but with $\epsilon' = 0.5$

Fig. 4(a). Γ_α versus θ. $\epsilon' = 2$. Solid curves for $l = 1$, $\epsilon'' = -0.001$, dashed curves for $l = 1$, $\epsilon'' = -0.5$, and dotted curves for $l = 5$, $\epsilon'' = -0.5$.

Fig. 4(b). Same as in Fig. 4(a) but with $\epsilon' = 0.5$

Fig. 5. Dependence of the components X_s and Y_s on θ in the vicinity of $\theta^{(c)}$. $\epsilon' = 0.5$ ($\theta^{(c)} = 45^o$), and $\epsilon'' = -0.001$. The thin, middle, and thick curves correspond to $l = 0, 1$, and 2, , respectively.

Fig. 6. Dependence of the components X_s and Y_s on ϵ' in the vicinity of $\epsilon' = \sin^2\theta$. $l = 1$, $\theta = 45^o$. The thick and thin curves correspond to $\epsilon'' = -0.001$ and $\epsilon'' = -0.01$, respectively.

Fig. 7. Dependence of the components X_s and Y_s on ϵ'' in the situation, when θ is close to $\theta^{(c)}$. $l = 1$, $\epsilon' = 0.5$. The thin and thick curves correspond to $\theta = 44.9^o = \theta^{(c)} - 0.1^o$ and $\theta = 45.1^o = \theta^{(c)} + 0.1^o$, respectively.

Fig. 8. Dependence of the components X_p and Y_p on θ in the vicinity of $\theta^{(B)}$. $\epsilon' = 2.0$ ($\theta^{(B)} = 54.7^o$), and $\epsilon'' = -0.001$. The thin and thick curves correspond to $l = 1$, and 2, respectively.

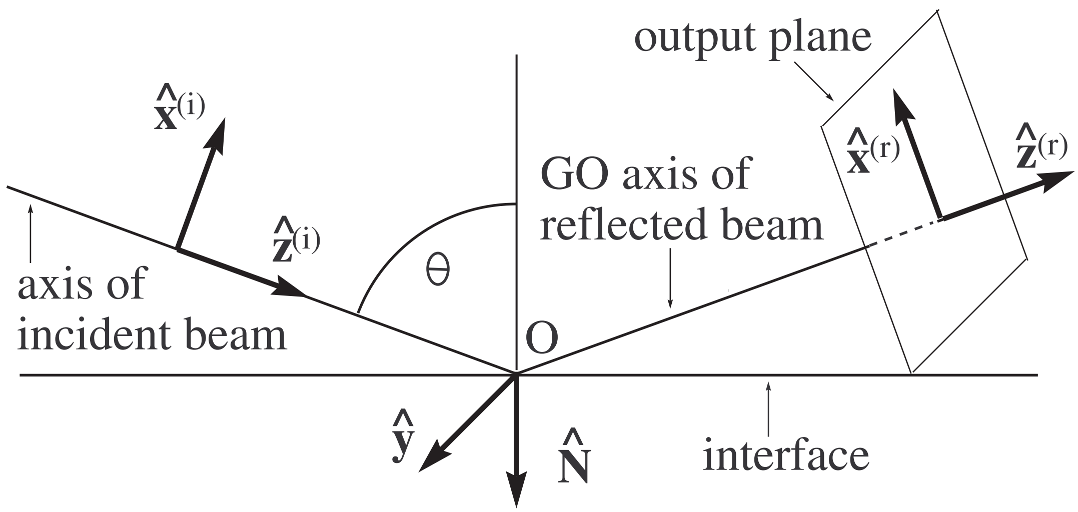

output plane
$\hat{x}^{(i)}$
$\hat{x}^{(r)}$
$\hat{z}^{(r)}$
GO axis of
reflected beam
$\hat{z}^{(i)}$
axis of
incident beam
Θ
O
$\hat{y}$
$\hat{N}$
interface

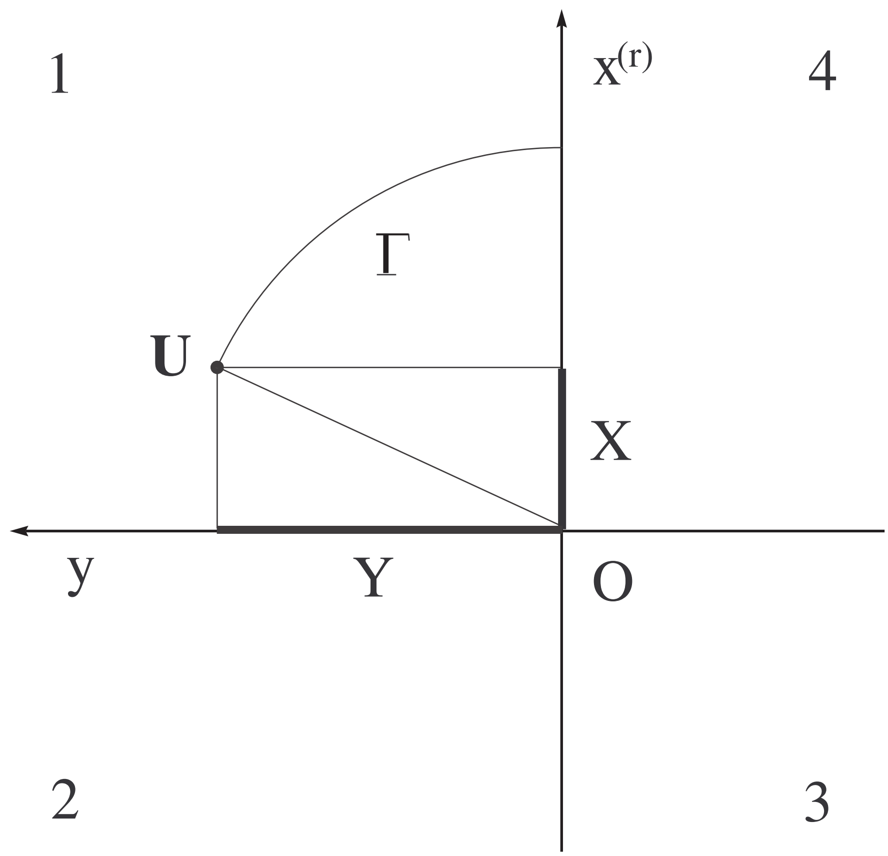

1
$x^{(r)}$
4
Γ
U
X
y
Y
O
2
3

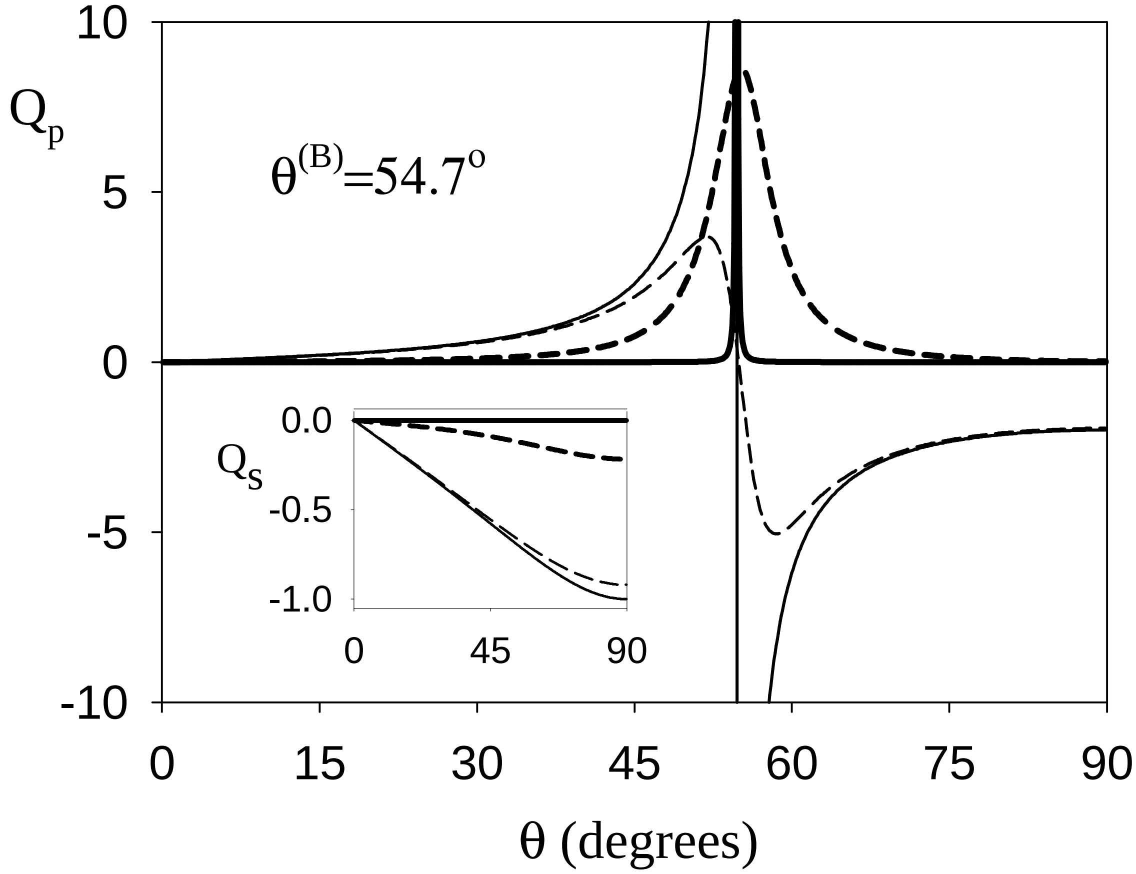

10
5
0
-5
-10
Q_p
$\theta^{(B)}=54.7^o$
0.0
-0.5
-1.0
Q_s
0
45
90
0
15
30
45
60
75
90
θ (degrees)

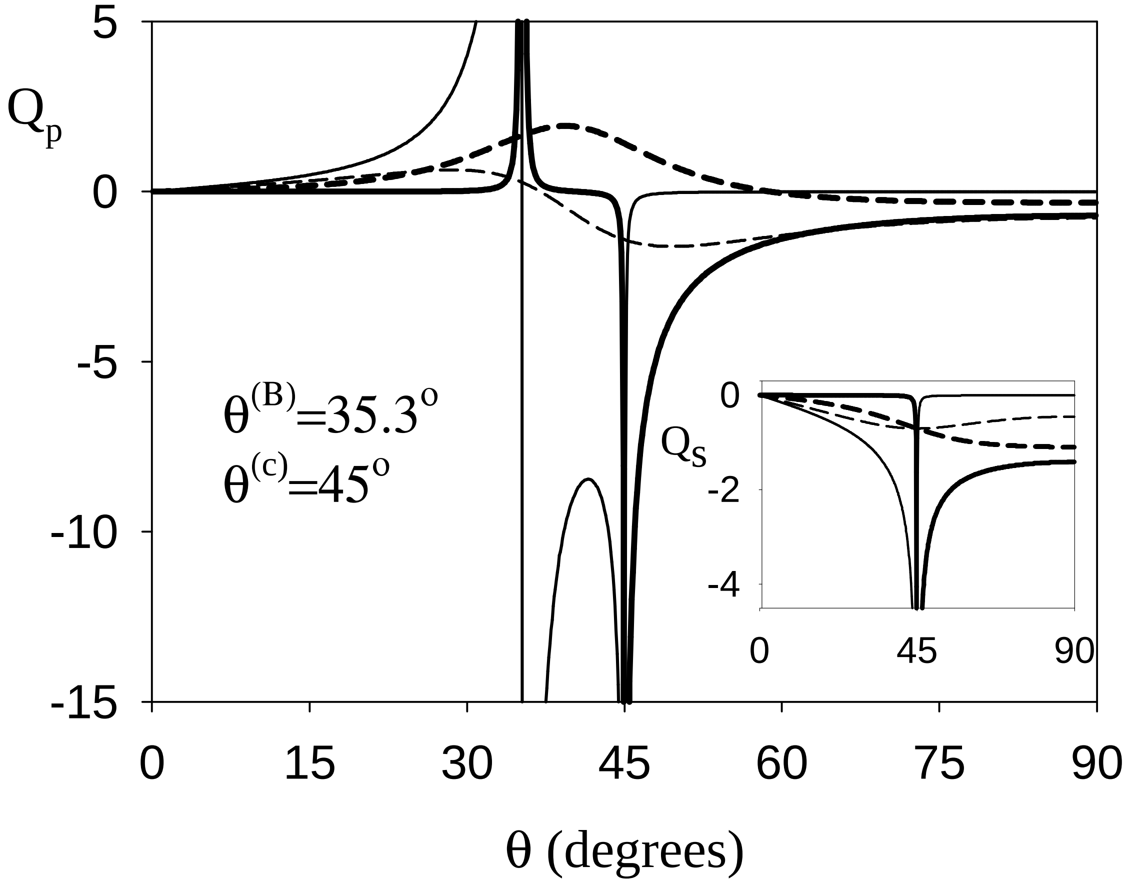

5
0
-5
-10
-15
Q_p
$\theta^{(B)}=35.3^o$
$\theta^{(c)}=45^o$
0
15
30
45
60
75
90
θ (degrees)
Q_S
0
-2
-4
0
45
90

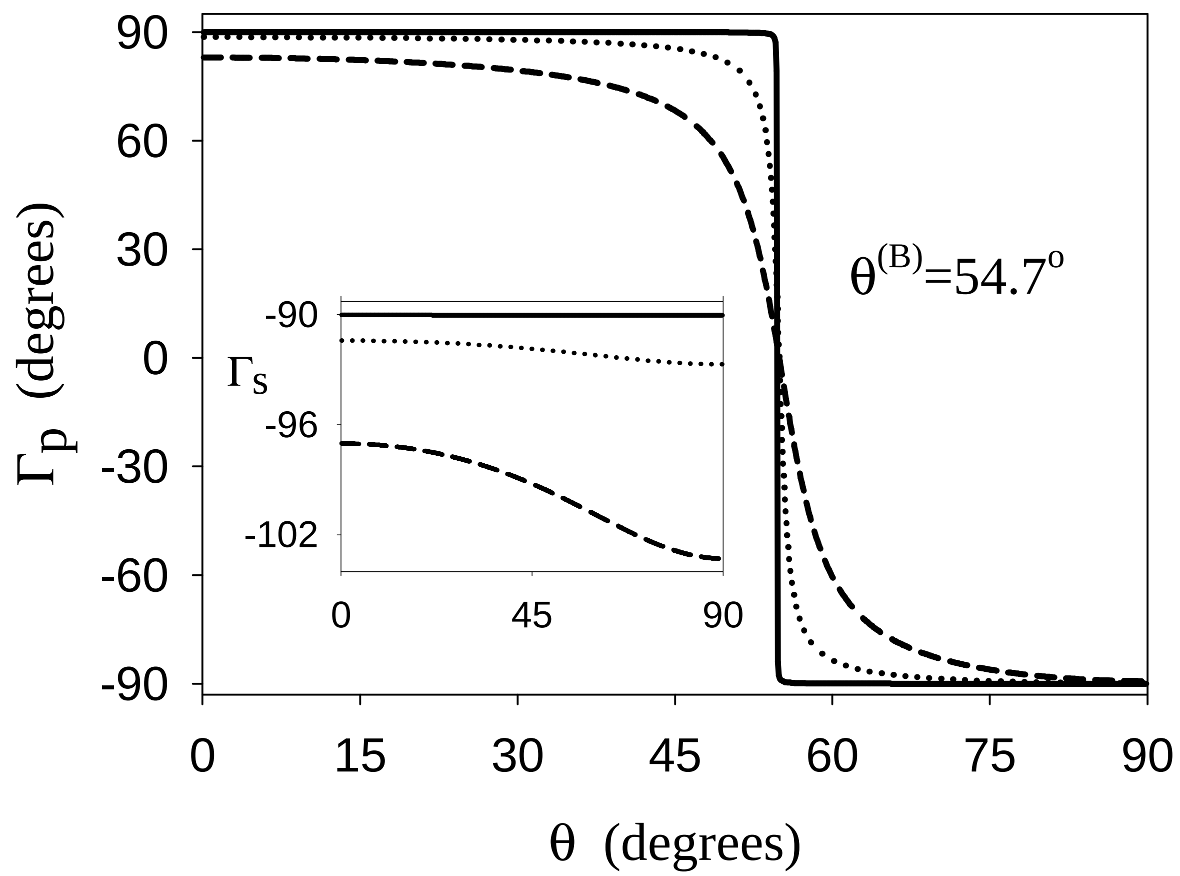

90
60
30
0
-30
-60
-90
Γp (degrees)
0
15
30
45
60
75
90
θ (degrees)
θ(B)=54.7o
-90
-96
-102
Γs
0
45
90

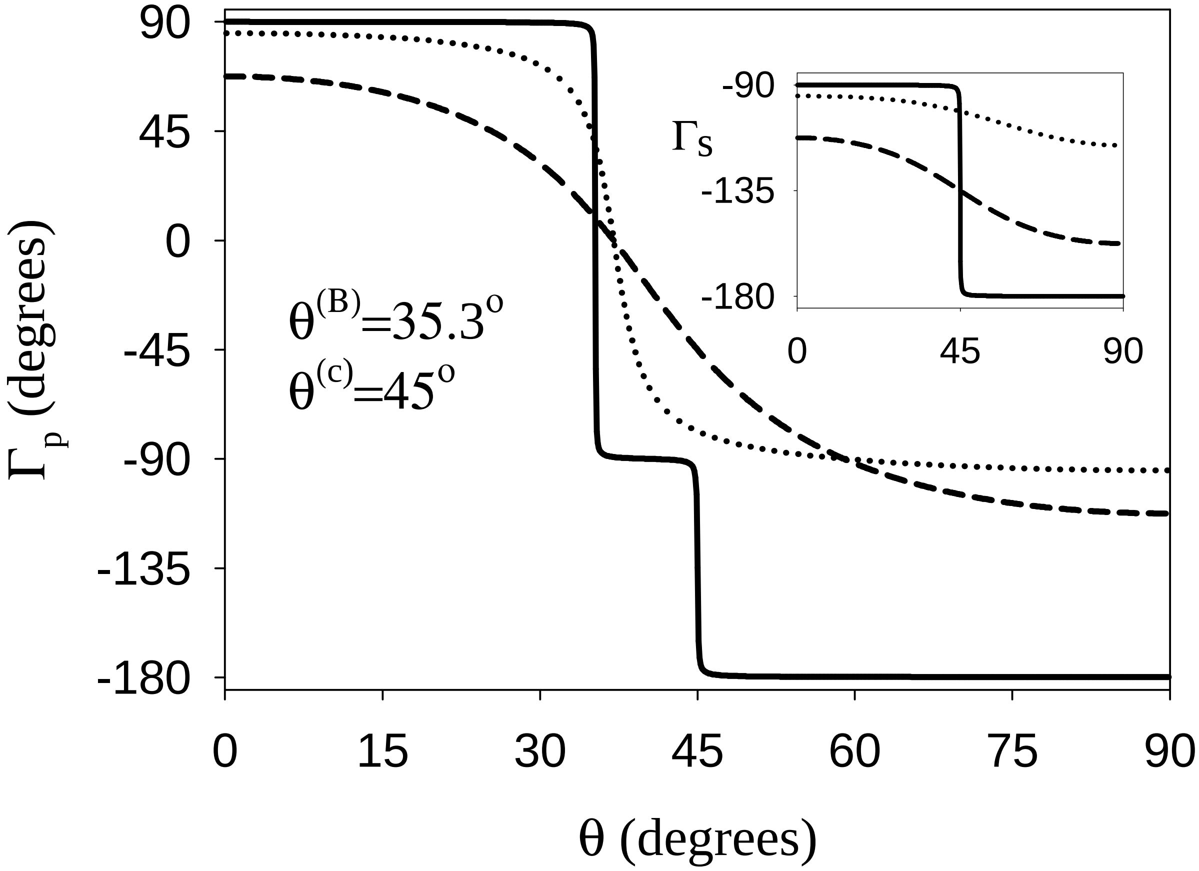

90
45
0
-45
-90
-135
-180
Γ_p (degrees)
$\theta^{(B)}$=35.3^o
$\theta^{(c)}$=45^o
-90
Γ_S
-135
-180
0
45
90
0
15
30
45
60
75
90
θ (degrees)

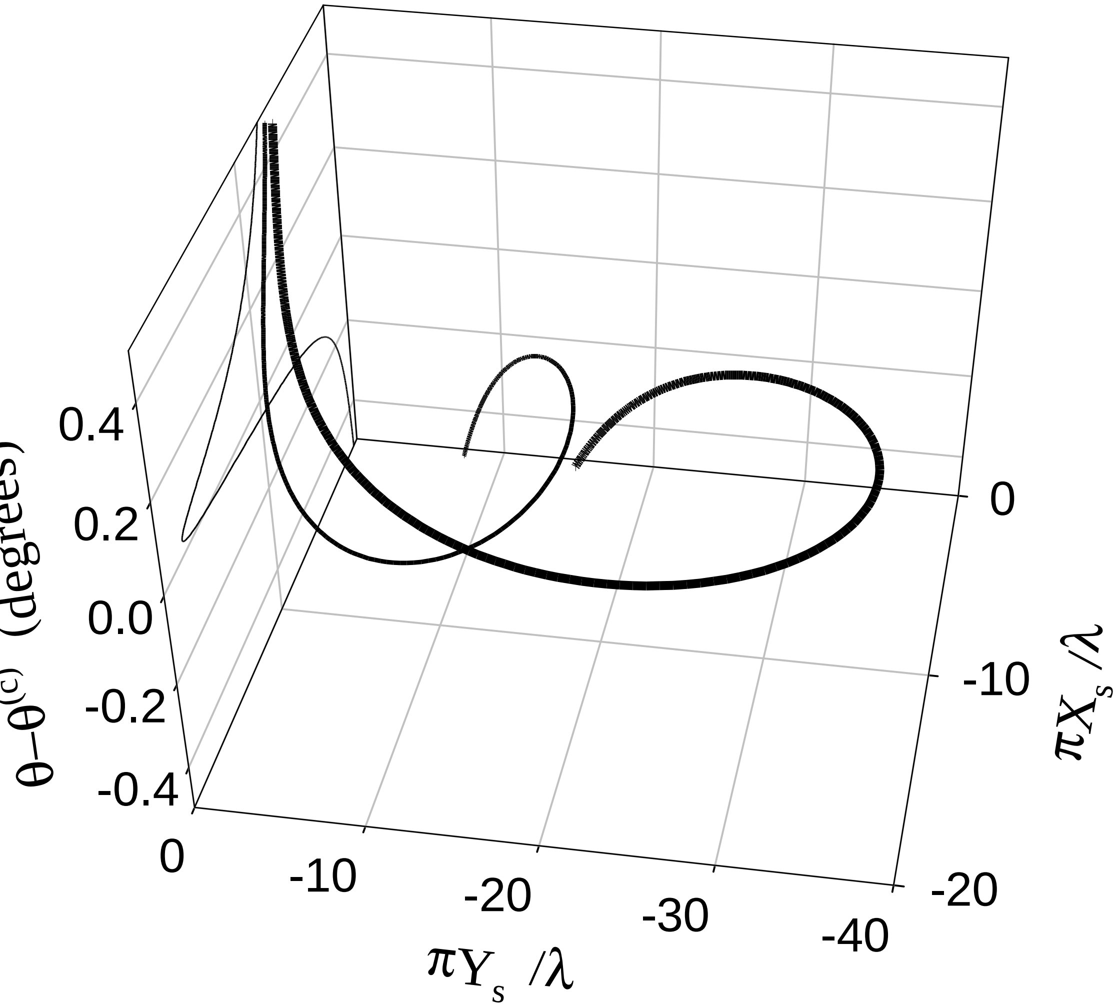

0.4
0.2
0.0
-0.2
-0.4
θ–θ(c) (degrees)
0
-10
-20
-30
-40
πYs /λ
0
-10
-20
πXs /λ

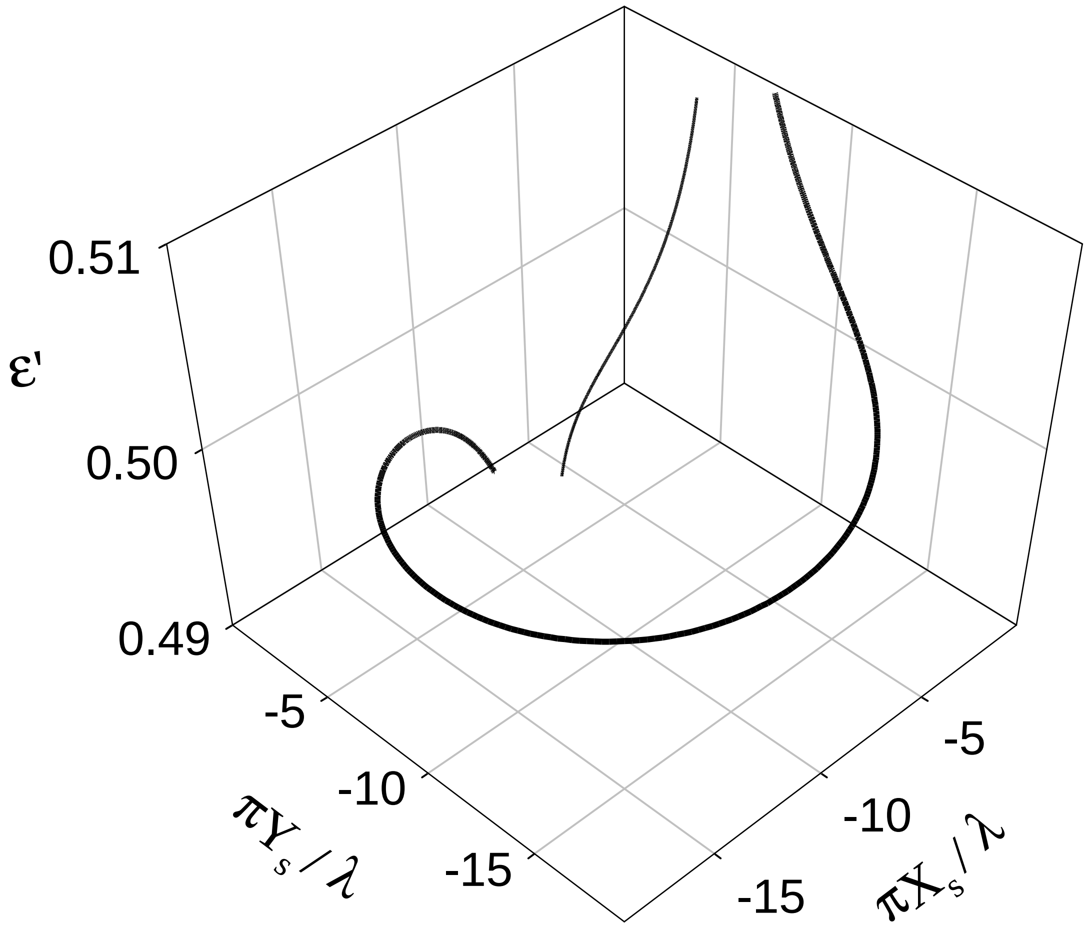

0.51
ε'
0.50
0.49
-5
-10
-15
$\pi Y_s / \lambda$
-5
-10
-15
$\pi X_s / \lambda$

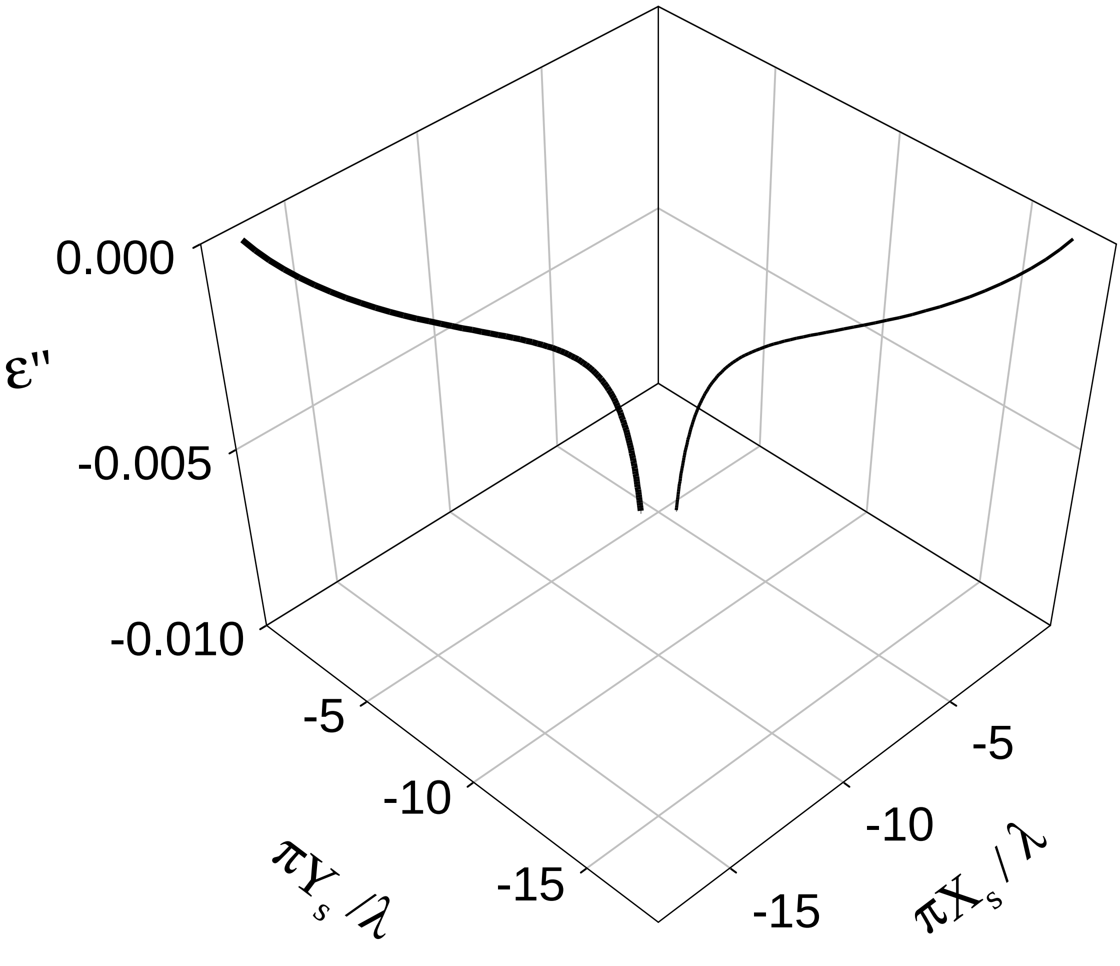

0.000
ε''
-0.005
-0.010
-5
-10
-15
πY_s /λ
-5
-10
-15
πX_s / λ

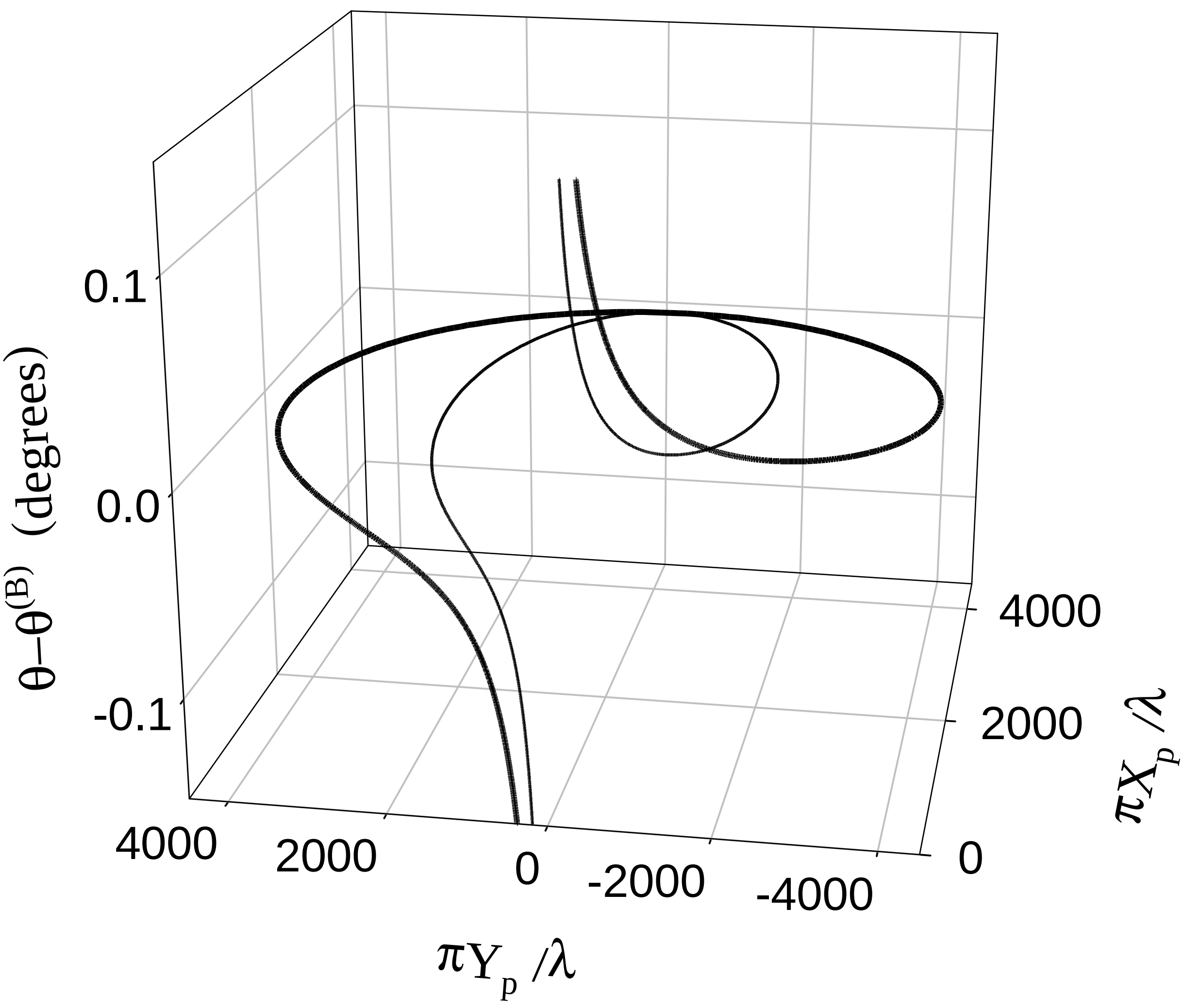
0.1
0.0
-0.1
θ–θ(B) (degrees)
4000
2000
0
-2000
-4000
πY_p /λ
4000
2000
0
πX_p /λ